Modulation of extraordinary optical transmission through nanohole arrays using ultrashort laser pulses

Kellie Pearce[a,b], Robin Dehde[a], Anika Spreen[a], Christian Späth[a], Maximilian Wendl[a], Jürgen Schmidt[a], Ulf Kleineberg[a]

[a]Faculty of Physics, Ludwig-Maximilians-Universität München, 85748 Garching, Germany; [b]Max Planck Institute of Quantum Optics, 85748 Garching, Germany

ABSTRACT

We use three dimensional finite-difference-time-domain simulations to study the dynamics of extraordinary optical transmission through arrays of nanoholes in 200 nm-thick Au films on silicon nitride substrates. By diving the light source into two identical 5 femtosecond pulses and tuning the relative delay between them, we are able to modulate both the intensity and spectra of the transmitted light on ultrashort time scales. Simulations demonstrate that the intensity and distribution of the electric fields on the surface of the film and within the nanoholes are altered by changing the pulse delay.

Keywords: Surface plasmons, extraordinary optical transmission

1. INTRODUCTION

Since its discovery in 1998[1], much progress has been made in investigating and understanding the phenomenon of extraordinary optical transmission (EOT). Ebbesen et al. first demonstrated that arrays of subwavelength holes in metal films can transmit visible light with efficiencies exceeding unity (when normalised to the holes' areas), which are orders of magnitude higher than the transmission predicted by classical diffraction theory[2]. In the subsequent two decades experiments and simulations have determined the effects of the properties of the metal film[1,3,4], the surrounding dielectric environment[5], the hole size and shape[6,7], the arrangement of the array[8], and the orientation of the incident light[9,10] on the transmission, as well as confirmed that surface plasmon polaritons play a major role[10,11]. Due to their transmissive properties and the presence of plasmonic fields on the surface, hole arrays in metal films have potential applications in novel photonic devices and biological sensing[12,13]. Examples of devices that have already been realised include wavelength filters[14,15], nanopolarilzers[16], and biosensors[17,18].

It has been shown that both localised surface plasmons around individual holes and surface plasmons polaritons (SPPs) travelling between the holes are present and affect the transmission[12,14]. Coupling between holes on and between the surfaces occurs on femtosecond time scales[19,20] and studying these dynamics is important to both our fundamental understanding of EOT and its application in photonic devices[21].

Compared with the large amount of research into the properties and potential applications of nanohole arrays, relatively few time-resolved studies have been carried out. One such early experiment used a setup based on linear interference to measure the transit time through an array and found a delay of 7 fs for a 300 nm film, which gives a group velocity of c/7[19,22]. This velocity can be much lower when the interface coupling is weak, giving longer delays of 60 – 100 fs[20]. Investigations into the temporal structure of the transmitted light have shown that the transmitted light is composed of two components - the original pulse, much is not greatly modified by the array, followed by a long, slowly decaying tail[21]. This structure stems from the interference between the direct, ultrafast transmission through the array, and the reradiation of light from plasmon modes on the surface. This Fano-type process is further evidenced by the point-spread function of the nanohole arrays[23] and the asymmetric lineshapes of the transmitted spectra[21,22]. Other time-resolved studies have found oscillations in the transmitted photon flux density[24], and SPP lifetimes of several hundred femtoseconds[21].

Given that our laser system is capable of producing ultrashort laser pulses of around 5 fs, we wish to exploit this high time resolution to study the dynamics of EOT with a pump-probe setup. To support our experiments and optimise the hole array parameters, we perform simulations to determine the effect of the second pulse on the transmission through the array and the evolution of the electric fields on the interfaces.

Nanophotonics VI, edited by David L. Andrews, Jean-Michel Nunzi, Andreas Ostendorf, Proc. of SPIE Vol. 9884, 98843H · © 2016 SPIE · CCC code: 0277-786X/16/$18 · doi: 10.1117/12.2228010

2. MATERIALS AND METHODS

Simulations are performed with Lumerical's 3D FDTD Solver. The simulation region centres on a unit cell of the two-dimensional hole array in the xy plane, as shown in Figure 1. The diameter of the hole *d* is kept at 200 nm. The square array is represented by a single nanohole centred in the simulation region, surrounded by periodic boundaries in the x and y directions which define the lattice constant *a* of the array. We choose a lattice constant of 650 nm, which gives transmission peaks within our excitation bandwidth. The thickness *h* of the metal film is 200 nm, ensuring its opacity in the absence of EOT, and is placed on a semi-infinite Si_3N_4 substrate to reduce the scattering and reflections that would be artificially introduced by a substrate of finite thickness. We select gold for the film material. The dielectric function of Au is taken from Johnson and Christy[25]; that of Si_3N_4 from Filmetrics, Inc.[26]. Choice of mesh size and accuracy, as well as the number of perfectly matched layers in the z-direction have been determined by using the convergence testing methods suggested by Lumerical.

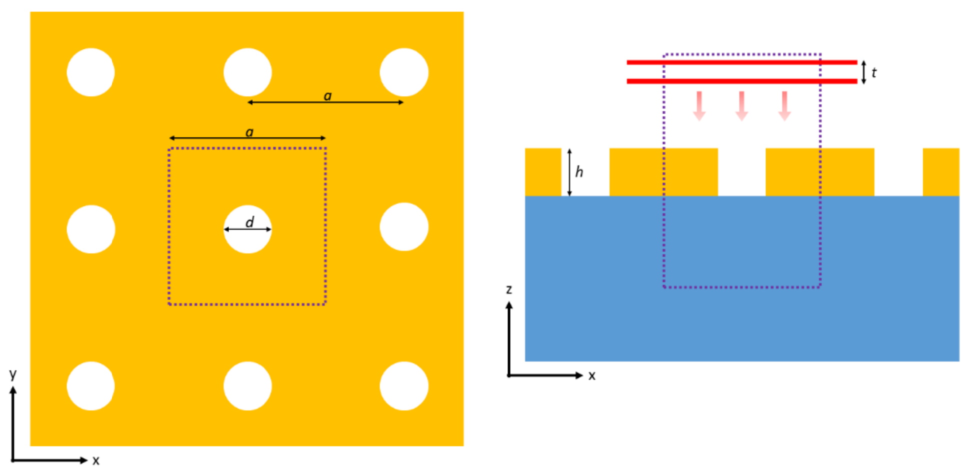

Figure 1. Illustration of the simulation setup. The simulation region is centred on a single hole of width *d* in a gold film of thickness *h*. The boundaries through the xy plane are periodic, so the span in the x- and y-directions defines the lattice constant *a*. The Au film rests atop a semi-infinite Si_3N_4 substrate. Two planar sources separated by a delay *t* are injected on the Au-vacuum side of the film and propagate in the -z direction.

Two sources are defined, which are identical in all parameters apart from relative offset *t*. Given that we expect our focal spot to be one to two orders of magnitude larger than the lattice constant of the array, the field over the simulation region can be regarded as uniform, so we choice plane wave sources, propagating in the negative z-direction and linearly polarized along the x-axis. The sources have a central wavelength of 760 nm with a span of 300 nm, and a pulse length of 5 fs. A starting offset of 20 fs for both pulses is chosen to ensure the pulse is not clipped in time. The total simulation time is 300 fs.

We place frequency- and time-domain monitors within the simulation region to record the transmitted spectra and the electric fields. Two planar frequency domain power monitors are situated on either side of the metal film, normal to the z-axis and some distance from the interfaces. These register the electric field passing through the plane in the time domain and carry out standard Fourier transforms, returning the transmitted spectra. An apodisation window is applied to elimate the first pulse from the Fourier transform, which gives incorrect results. The simulations are performed in the continuous wave normalisation state. Frequency-domain profile monitors are placed in the xz plane at y=0 and in the xy plane at the Au/Si_3N_4 interface to record the electric field profiles at specified wavelengths. Two point time-domain monitors placed in the centre of the hole and on the metal-substrate interface midway between two holes return the electric field at these points as a function of time. In addition, two two-dimensional time-domain monitors are placed in the same locations as the frequency-domain profile monitors.

3. RESULTS AND DISCUSSION

The transmission spectra for the array at several time delays are shown in Figure 2. At zero delay, two transmission peaks occur at 698 nm and 757 nm. At this lattice spacing and excitation wavelengths, the mechanism for transmission contains contributions from both localised and SPP resonances, with the relative contributions from each decreasing and increasing, respectively, with larger lattice spacings[27].

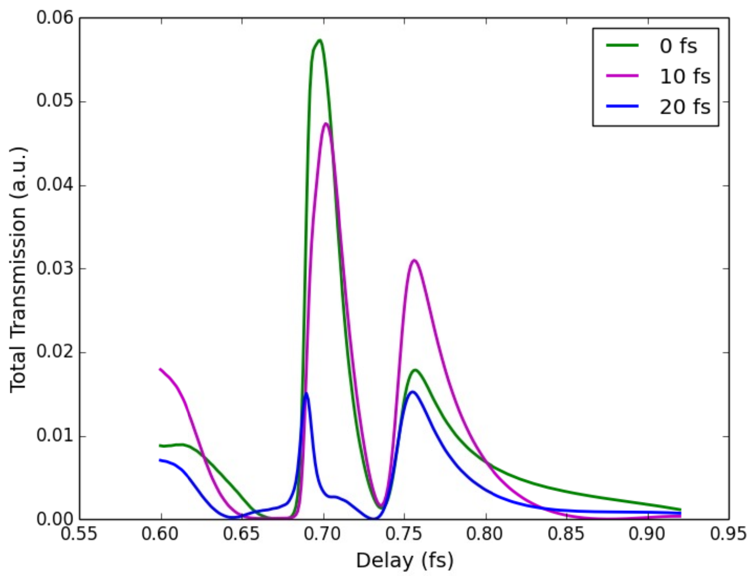

Figure 2. Transmission spectra of the array for various time delays between the pulses.

Spectra are also shown at time delays of 10 and 20 fs. The presence of a second, delayed pulse modifies both the intensity and spectral distribution of the transmitted light. The transit time for the pulses is 4.9 – 5.9 fs, depending on lattice configuration, consistent with earlier results[19]. The peak at 698 nm displays a profound change in intensity when the pulse delay is altered, as well as a shift in the peak wavelength. The change in the peak at 757 nm is less pronounced, but still sizeable. Simulations using other lattice spacings (not discussed here) suggest that this second peak is due to localised excitations around the holes, so the second pulse primarily affects that component of EOT that is due to interhole coupling.

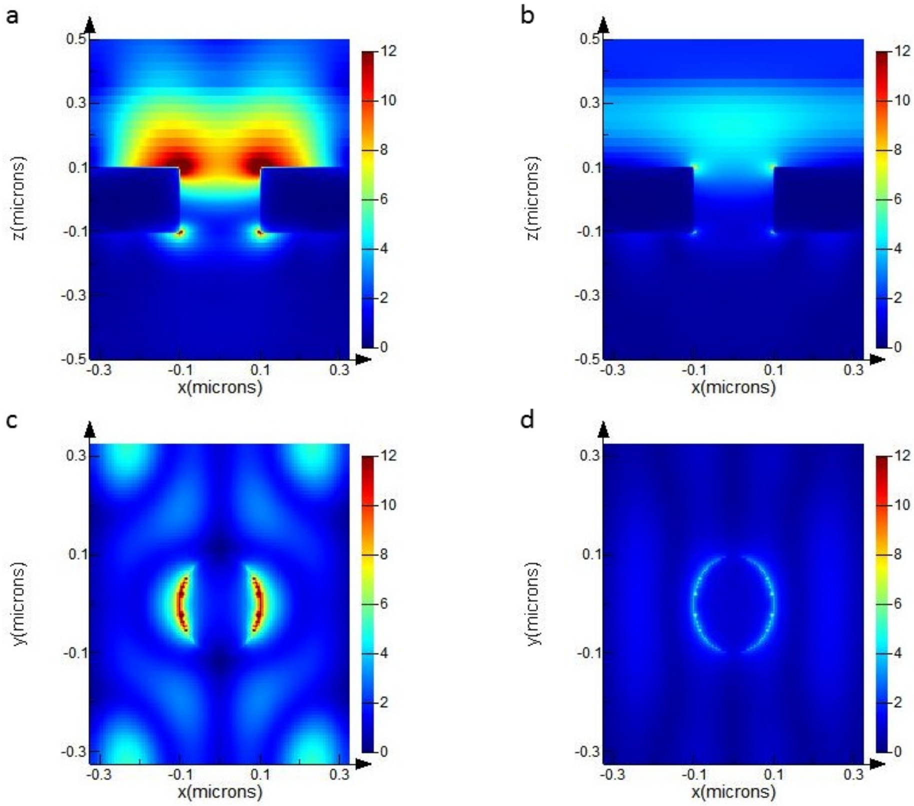

Figure 3. Frequency-domain profile monitors of the magnitude of the electric field for the peaks at a), c) 698 nm and b), d) 757 nm. A cross-section of the film through y=0 is shown in a) and b); c) and d) show the underside of the film at the Au/Si_3N_4 interface

Profiles of the electric fields in the frequency domain at the two peak wavelengths are shown in Figure 3. Figures 3a and 3b show the magnitude of the electric fields through a cross section of the film at 698 and 757 nm, respectively. Figures 3c and 3d show the fields on the underside of the film at the Au/Si_3N_4 interface. The 698 nm peak displays stronger, more directional fields around the hole edge, while the hole edge of the 757 nm peak is more uniformly enhanced and the fields are weaker. On the underside of the film, the fields at 698 nm are stronger and form a more complex pattern, indicating interference of propagating modes.

Figure 4 shows the results from the two point time-domain monitors in the hole and on the Au/Si_3N_4 interface. Figure 4a shows the value of the x-component of the electric field, recorded in the centre of the hole. With zero delay between the two excitation pulses, the incoming pulse is seen, followed by a long, decaying tail, evident of the resonant nature of the cylindrical hole. For a 10 fs pulse delay, the fields of the individual pulses are seen, while the resonance is somewhat supressed.

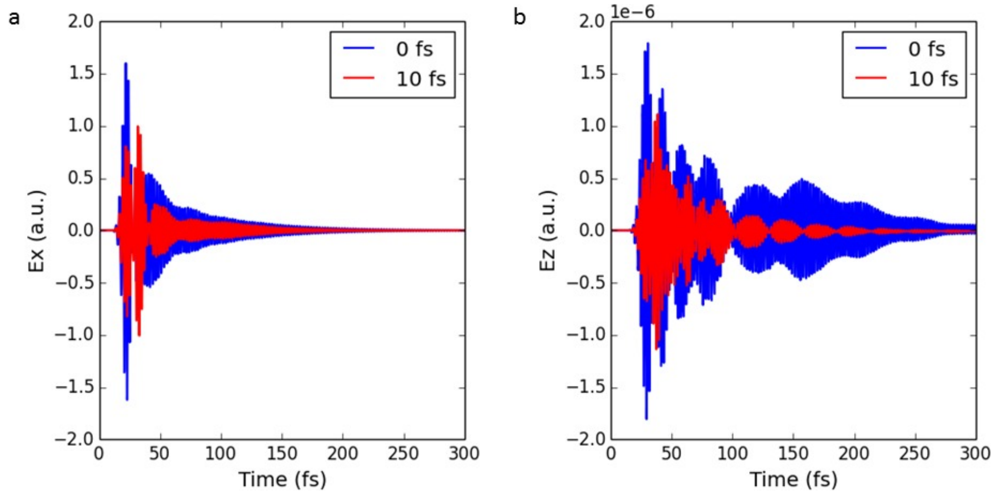

Figure 4. Evolution of the electric fields at two points in the array for two different time delays between the pulses. a) The x-component of the electric field in the centre of the hole. b) The z-component of the electric field on midway between the holes on the Au/Si_3N_4 interface.

Figure 4b shows the z-component of the electric field at a point mid-way between two holes on the underside of the film. Given that the electric fields of the initial pulses have only x-components, these fields can be only due to the presence of plasmons on the surface. We therefore attribute the strong beating pattern to the interference of plasmons originating from different holes in the film. The second pulse clearly modifies the frequency of the beating and leads to a faster decay of the fields.

Snapshots of the total electric field profile through a cross-section of the film at y = 0 at times of 24, 40, and 60 fs (4, 20, and 40 fs after injection of the pulses) are shown in Figure 5. The top row (a-c) shows the fields for a delay of 0 fs between the pulses at each of these three simulation times. After 4 fs (left image) the incident field has reached the top surface of the film, producing localised enhancement around the hole edge. At 20 fs (middle image), the field has begun to resonate inside the hole, and the hole edge on the underside of the film shows field enhancement. At 40 fs (right image), the SPP on the underside of the film can be seen. The bottom row (d-f) shows the fields at the same simulation times but with the second pulse arriving after a delay of 10 fs. These images reinforce the observation that the second pulse modifies the time signature of the fields.

4. CONCLUSIONS

We have performed FDTD simulations of the transmission of ultrashort laser pulses through a square array of nanoholes in an Au film on a Si_3N_4 substrate. The transmission spectrum displays two prominent peaks, seemingly due to SPP and LSP resonances. Introducing a time delay between the two identical incident laser pulses modifies the peak intensity and spectral position. Results from measurements of the electric fields indicates that the second pulse influences the SPP resonance and damping rate. This offers the possibility to modulate the transmission spectra and local fields of a nanohole array on femtosecond time scales, both of which could be used in applications.

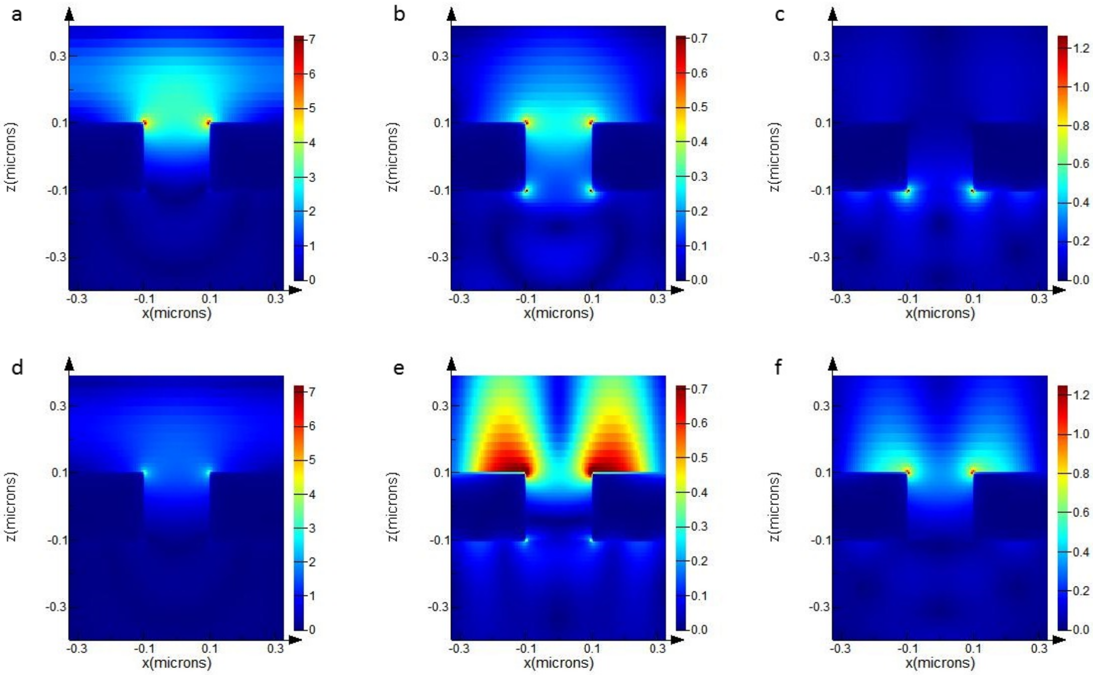

Figure 5. Two-dimensional time monitors showing electric field magnitude at several simulation times. Snapshots of the fields at 4, 20, and 40 fs after the first and second pulses are simultaneously injected are shown in a) – c). Snapshots of the fields at the same simulation times but with a 10 fs delay for the second pulse are shown in d) – f).

REFERENCES

[1] Ebbesen, T. W., Lezec, H. J., Ghaemi, H. F., Thio, T., Wolff, P. A., "Extraordinary optical transmission through sub-wavelength hole arrays," Nature 391, 667-669 (1998)

[2] Bethe, H. A., "Theory of Diffraction by Small Holes," Phys. Rev. 163, 163-182 (1944)

[3] Przybilla, F., Degiron, A., Laluet, J-Y., Gennet, C., Ebbesen, T. W., "Optical transmission in perforated noble and transition metal films," J. Opt. A: Pure Appl. Opt 8, 458-463 (2006)

[4] Rodrigo, S. G., García-Vidal, F. J., Martín-Moreno, L., "Influence of material properties on extraordinary optical transmission through hole arrays," Phys. Rev. B 77, 075401 (2008)

[5] Krishnan, A., Thio, T., Kim, T.J., Lezec, H. J., Ebbesen, T. W., Wolff, P. A., Pendry, J., Martín-Moreno, L., García-Vidal, F. J., "Evanescently coupled resonance in surface plasmon enhanced transmission," Opt. Commun. 200, 1-7 (2001)

[6] Koerkamp, K. J., Segerink, F. B., van Hulst, N. F., Kuipers, L., "Strong influence of hole shape on extraordinary optical transmission through periodic arrays of subwavelength holes," Phys. Rev. Lett. 92, 183901 (2004)

[7] van der Molen, K. L., Segerink, F. B., van Hulst, N. F., "Influence of hole size on the extraordinary transmisison through subwavelength hole arrays," App. Phys. Lett. 85, 4316-4318 (2004)

[8] Przybilla, F., Genet, C., Ebbesen, T. W., "Enhanced transmission through Penrose subwavelength hole arrays," App. Phys. Lett. 89, 121115 (2006)

[9] Ghaemi, H. F., Thio, T., Grupp, D. E., Ebbesen, T. W., Lezec, H. J., "Surface plasmons enhance optical transmission through subwavelength holes," Phys. Rev. B 58, 6779-6782 (1998)

[10] Degiron, A., Ebbesen, T. W., "The role of localized surface plasmon modes in the enhanced transmission of periodic subwavelength apertures," J. Opt. A, Pure Appl. Opt. **7**, S90-S96 (2005)

[11] Gao, H., Henzie, J., Odom, T. W., "Direct evidence for surface plasmon-mediated enhanced light transmission through metallic nanohole arrays," Nano Lett. 6, 2104-2108 (2006)

[12] García-Vidal, F. J., Martín-Moreno, L., Ebbesen, T. W., Kuipers, L., "Light passing through subwavelength apertures," Rev. Mod. Phys. 82, 729-787 (2010)

[13] Ropers, C., Elsaesser, T., Cerullo, G., Zavelani-Rossi, M., Lienau, C., "Ultrafast optical excitations of metallic nanostructures: from light confinement to a novel electron source," New J. Phys. 9, 397 (2007)

[14] Genet, C., Ebbesen, T. W., "Light in tiny holes," Nature 445, 39-46 (2007)

[15] Lee, H. S., Yoon, Y. T., Lee, S. S., Kin, S. H., Lee, K. D., "Color filter based on a subwavelength patterned metal grating," Opt. Exp. 15, 15457-15463 (2007)

[16] Onishi, T., Tanigawa, T., Ueda, T., Ueda, D., "Polarization control of vertical-cavity surface-emitting lasers by utilizing surface plasmon resonance," IEEE J. Quantum Electron. 43, 1123 (2007)

[17] Cooper, M., "Optical biosensors in drug discovery," Nat. Rev. Drug Discovery 1, 515-528 (2002)

[18] Brolo, A. G., Gordon, R., Leathem, B., Kavanagh, K. L., "Surface plasmon sensor based on the enhanced light transmission through arrays of nanoholes in gold films," Laser & Photon. Rev. 20, 4813 (2004)

[19] Dogariu, A., Thio, T., Wang, L. J., Ebbesen, T. W., Lezec, H. J., "Delay in light transmission through small apertures," Opt. Lett. 26, 450-452 (2001)

[20] Su, H. M., Hang, Z. H., Marcet, Z., Chan, H. B., Chan, C. T., Wong, K. S., "Propagation dynamics of femtosecond pulse through subwavelength metallic hole arrays," Phys. Rev. B 83, 245449 (2011)

[21] Ropers, C., Stibenz, G., Steinmeyer, G., Müller, R., Park, D. J., Lee, K. G., Kim, J., Park, Q. H., Kim, D. S., Lienau, C., "Ultrafast dynamics of surface plasmon polaritons in plasmonic metamaterials," Appl. Phys. B 84, 183-189 (2006)

[22] Kim, D. S., Hohng, S. C., Malyarchuk, V., Yoon, Y. C., Ahn, Y. H., Yee, K. J., Park, J. W., Kim, J., Park, Q. H., Lienau, C., "Microscopic origin of surface-plasmon radiation in plasmonic band-gap nanostructures," Phys. Rev. Lett. 91, 143901 (2003)

[23] Altewischer, E., Ma, X., van Exter, M. P., Woerdman, J. P., "Fano-type interference in the point-spread function of nanohole arrays," Opt. Lett. 30, 2436-2438 (2005)

[24] Mueller, R., Malyarchuk, V., Lienau, C., "Three-dimensional theory on light-induced near-field dynamics in a metal film with a periodic array of nanoholes," Phys. Rev. B 68, 205415 (2003)

[25] Johnson, P. B., Christy, R. W., "Optical constants of the noble metals," Phys. Rev. B 6, 4370 (1972)

[26] "Brechungsindex von Silicon Nitride," Filmetrics, Inc., <http://www.filmetrics.de/refractive-index-database/Si3N4/Silicon-Nitride-SiN> (25 August 2015)

[27] Mary A, Rodrigo, S. G., Martín-Moreno, L., García-Vidal, F. J., "Theory of light transmission through an array of rectangular holes," Phys. Rev. B 76, 195414 (2007)